E-Journal of Advanced Maintenance Vol.5-1 (2013) 42-50
Japan Society of Maintenology

# Simplified Electromagnetic Inverse Analysis Technique about the Inclined Defect for Welded Zone of High Chromium Steel

Shogo NAKASUMI[1,*], Takayuki SUZUKI[1], Naoyuki TAKASHIMA[2] and Yuji TSUCHIDA[3]

[1] *National Institute of Advanced Industrial Science and Technology, East 1-2-1 Namiki, Tsukuba, Ibaraki 305-8564, Japan*
[2] *University of Tsukuba, Tennodai 1-1-1, Tsukuba, Ibaraki, 305-8573, Japan*
[3] *Oita University, 700, Dannoharu, Oita-shi, Oita, 870-1192, Japan*

**ABSTRACT**

A simplified technique of obtaining the shape of inclined defect at welded zone of high chromium steel was proposed. Magnetic flux leakage measurement and the inverse analysis using singular value decomposition were used. From the magnetic flux density distribution obtained under the high magnetic field, adequate defect shape was obtained without the influence of welded zone. Under the low magnetic field, adequate defect shape was obtained by subtracting the magnetic field of welded zone from measured magnetic flux distribution.

**KEYWORDS**

inclined defect, magnetic flux leakage, welded zone, inverse analysis, magnetic dipole moment

**ARTICLE INFORMATION**

*Article history:*
*Received 17Nobember 2012*
*Accepted 12 March 2013*

## 1. Introduction

In recent years, the high accuracy evaluation technique of degradation and damages in industrial plants such as fast breeder reactor “Monju” has been studied for safety and reliability. In case of using a ferromagnetic material like high chromium steel for structural members of nuclear instrument as weld joint, inclined defects and damages often occur in the Heat Affected Zone (HAZ) around welded zone as shown in Fig.1. Difference of material and the shape of inclined defects have complicated influence on the distribution of magnetic flux density.

To detect the defect, magnetic flux leakage (MFL) technique is one of the non-destructive evaluation (NDE) methods for ferromagnetic structural materials [1]. In MFL, defects are detected by measuring the magnetic flux leakage caused by the magnetic charges on the defect surfaces. Sensors for measuring MFL are Hall sensors, flux gate sensors [2], SQUID and so on.

In numerical simulation of MFL, defects can be represented by using magnetic dipoles on the defect plane, and the defect shape is estimated by conducting the inverse analysis. This technique has been studied by several researchers. For example, Minkov *et al*. used the analytically integrated expression of magnetic field of a parallelepiped surface crack, and they estimated the width and depth of the crack [3,4]. Baskaran and Janawadkar detected bar shape defects [5], and they identified the positions and magnitude of the magnetic dipoles using the orthogonally projected MUSIC (MUltiple SIgnal Classification) algorithm based on pseudo-inverse technique [6,7,8]. Nakasumi and Suzuki improved the function which associates the magnetic dipoles and magnetic flux so as to capture the average value of magnetic flux along the sensor length, and they showed the effect by inverse analysis of Tikhonov regularization technique using single crack models [9] and multiple crack models [10]. However, targets of these researches are simple shape defects in homogeneous material, and the inverse analysis for inclined defects in unhomogeneous material such as welded parts has not been conducted.

In this study, therefore, the inclined defect of Type-III around HAZ of high chromium steel welded zone is focused on as practical structural parts. Although the Type-IV defect is also important

*Corresponding author, E-mail: nakasumi.shogo@aist.go.jp

for practical purpose, NDE using magnetic flux leakage is considered to be suited for Type-III better than Type-IV, because the magnetic flux decreases steeply as the distance between the defect and the sensor becomes large. Then, we will present the simple approach for defect shape evaluation using inverse analysis.

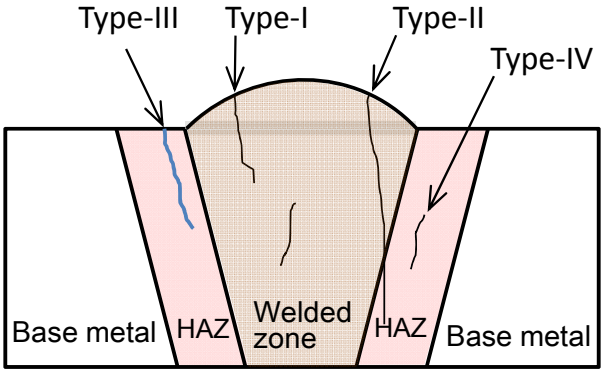


**Fig. 1. Type of defects around HAZ of weld joint**

## 2. Theoretical background of inverse analysis for inclined defect

### 2.1. Representation of defects using magnetic dipole moments

In this section, we will set the relationship between defect shape and magnetic flux distribution. Figure 2 shows the conceptual model with an inclined defect. The defect is rectangular shape and it is inclined to angle $\theta$ from the perpendicular line. Magnetic dipoles are configured in lattice pattern on that inclined plane. We assumed that the magnitude of magnetic density on the defect is uniform. Therefore, magnetic dipoles are configured at regular intervals, and the magnitude of them on the defect is constant. As for this, some researchers assume that the magnitude of magnetic dipoles change linearly in the depth direction [3]. However, the purpose of this inverse analysis is to estimate the defect shape. Therefore, for inverse analysis, it is not necessary to obtain the physically precise distribution of magnet.

The defect is represented by magnetic dipole moments as shown in Figure 2, and we assume that the direction of magnetic dipole is fixed to be that of y-axis, regardless of the inclination angle of the defect. The magnetic flux density observed at the point is given by Eq. (1) [9, 10].

$$B_y(\mathbf{x}) = \sum F_y(\mathbf{x}-\mathbf{x}')m_y \tag{1}$$

Here, the point $\mathbf{x}' = (x', y', z')^T$ is the coordinate of magnetic dipole on the defect plane, $N$ is the total number of the magnetic dipoles, $m_y$ is density of magnet, and $F_y(\mathbf{x})$ is the response function which is denoted by Eq. (2).

$$F_y(x,y,z) = \mu_0\left(x^2+y^2-2z^2\right)\Big/ 4\pi\left(x^2+y^2+z^2\right)^{5/2} \tag{2}$$

Here, $\mu_0$ is the magnetic permeability of vacuum. Eq. (1) holds at every observation point when the observation point varies on the plane that maintains a certain constant liftoff value. Finally, we obtain a matrix equations of Eq. (3). Here, **B** and **m** are vectors which are obtained by setting the observation points and magnet dipoles, respectively. **F** is a matrix, which is composed of $F_y$ in Eq. (2).

$$\mathbf{B} = \mathbf{Fm} \tag{3}$$

## 2.2. Procedure of inverse analysis using singular value decomposition technique

The defect shape, namely the value of magnetic dipoles $\mathbf{m}$ of equation (3) is derived from the

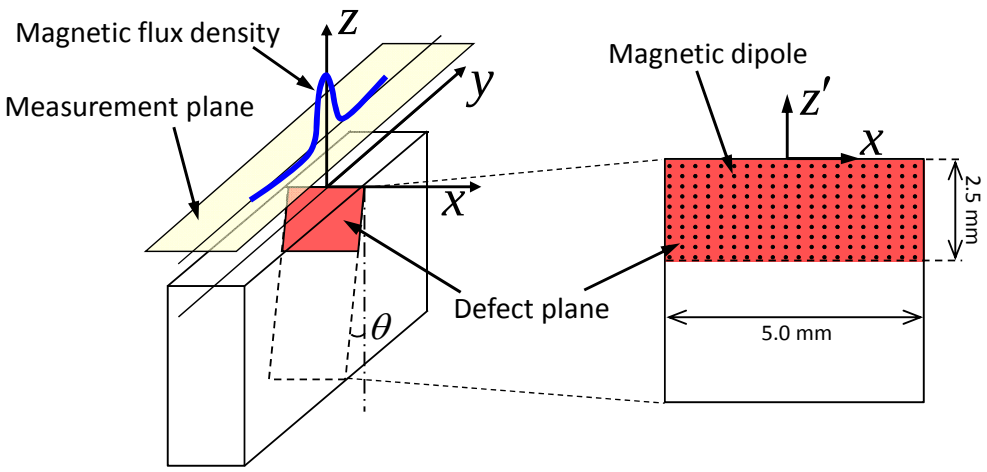


**Fig. 2. Defect and coordinate system**

magnetic flux distribution $\mathbf{B}$ by the inverse analysis. However, $\mathbf{F}$ of equation (3) often becomes ill-posed condition matrix, and so-called vibration solutions are often obtained.

To avoid this difficulty, Tikhonov regularization technique [11] or Singular Value Decomposition (SVD) technique are often used. As for the Tikhonov regularization technique, however, arbitrariness of the formulation of regularization term occurs, and this makes the interpretation of the solution of inverse analysis unclear. In this work, therefore, we use the SVD technique, and thus we can avoid that arbitrariness. We will briefly explain the formulation below. The matrix $\mathbf{F}$ is generally decomposed like following formula.

$$\mathbf{F} = \sum_{i=1}^{r} \lambda_i \mathbf{u}_i \mathbf{v}_i^T \tag{4}$$

Here, $\lambda_i$ is the $i^{\text{th}}$ singular value, $\mathbf{u}_i$ and $\mathbf{v}_i^T$ are the left and the right singular vectors corresponding to $\lambda_i$ respectively. And, $r$ is the total number of singular values. From equation (3) and equation (4), we can obtain the solution $\bar{\mathbf{m}}$ as equation (5).

$$\bar{\mathbf{m}} = \sum_{i=1}^{r} \frac{\mathbf{v}_i \mathbf{u}_i^T}{\lambda_i} \mathbf{B} \tag{5}$$

Usually, noises, such as errors of measurement, are contained in magnetic flux density. Therefore, equation (5) means that the noises contained in the measured magnetic flux density is amplified by the singular value of quite small size, and this reduces remarkably the accuracy of inverse analysis. To avoid this, therefore, we set the threshold value $\lambda_k \ (1 < k < r)$ to $\lambda_i$, and we truncate the singular values smaller than $\lambda_k$. Namely, $\bar{\mathbf{m}}$ is represented like equation (6).

$$\bar{\mathbf{m}} = \sum_{i=1}^{k} \frac{\mathbf{u}_i \mathbf{v}_i^T}{\lambda_i} \mathbf{B} \quad (1 < k < r) \tag{6}$$

By this operation, the information of high-frequency component which corresponds to more than $(k+1)^{\text{th}}$ singular value is lost from the whole solution space. However, since the noise effect contained in this area is also removed, we can expect to obtain the stable solution.

However, since the important information is lost if the threshold value $\lambda_k$ is too large, we need to be cautious of determining it. We used so-called L-curve approach [12]. Namely, as $\lambda_k$ enlarges from zero, we can obtain a L-shape curve by plotting points to the plane whose horizontal and vertical axes are the residual term norm ($\|\mathbf{Fm}-\mathbf{B}\|$) and the solution vector norm ($\mathbf{m}$), respectively. Generally speaking, it is thought the $\lambda_k$ that corresponds to the kink of this curve gives the most appropriate distribution of magnetic dipoles. That is to say, the threshold value $\lambda_k$ which makes both the residual norm and the solution norm simultaneously minimized gives the most suitable solution.

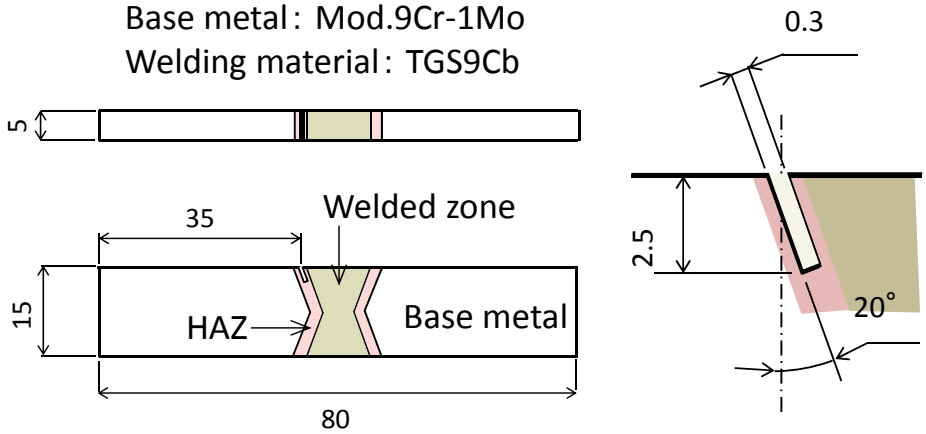


**Fig. 3. Specimen with an inclined defect**

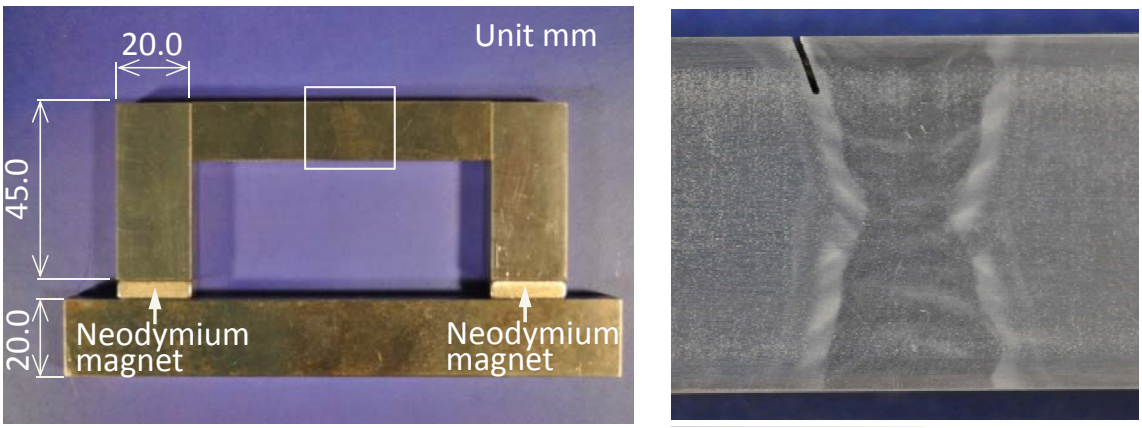


**(a) Overall view** **(b) Enlarged view of inclination defect and welded zone**

**Fig. 4. Magnetization setup**

## 3. Inverse analysis using experimental magnetic flux data of inclined defect

### 3.1. Specimen and magnetization

Figure 3 shows the specimen used in this study. It was obtained from the high chromium (Mod.9Cr-1Mo) steel welded specimen. On the boundary of a welded zone layer and HAZ, the defect of 2.5 mm depth and inclined angle of 20 degree was prepared in parallel with weld line by wire cutting. In order to compare the magnetic flux density distribution by the difference of magnetization conditions, the specimen was magnetized using two kinds of magnets, neodymium magnets (surface -inductive-flux $4.88\times10^{-1}$T) and ferrite magnets (the $1.33\times10^{-1}$T).

Figure 4 shows the setup for magnetization of the specimen. The specimen was magnetized in a longitudinal direction using the yoke with two neodymium magnets. The magnetic flux density around the tip of the yoke was $4.88\times10^{-1}$T when the neodymium magnets were attached to the yoke.

### 3.2. Measurement system

Figure 5 shows the experimental setup for magnetic flux density measurement. A hall sensor is used to capture the magnetic flux density at the distance of liftoff. Resolution of this hall sensor is $1.0\times10^{-5}$T . Magnetic flux leakage was measured along on six layers in the direction of longitudinal. Liftoff is set to be 1 mm and the interval of measurement is 0.1 mm in x-axis direction, and 1 mm in y-axis direction.

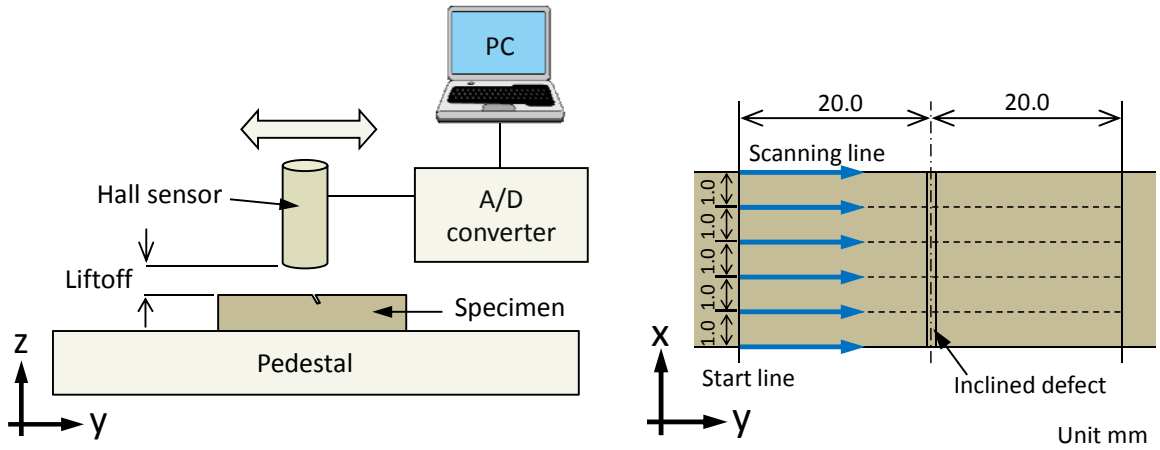


**(a) Experimental setup** **(b) Scanning line**

**Fig. 5. Measurement system**

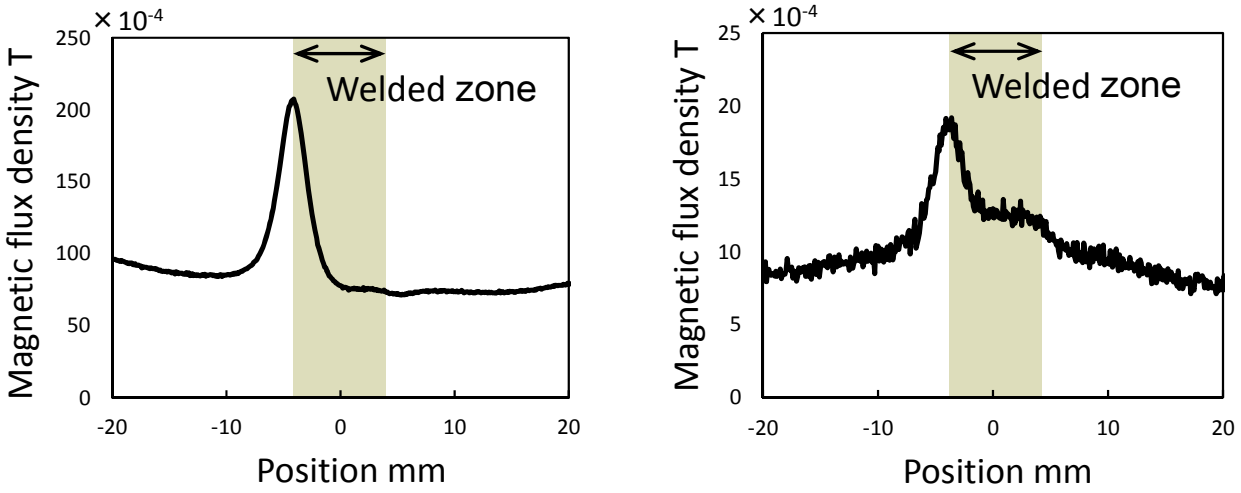


**(a) Applied magnetic field $4.88\times10^{-1}$T** **(b) Applied magnetic field $1.33\times10^{-1}$T**

**Fig. 6. Magnetic flux leakage distribution**

### 3.3. Inverse analysis using original experimental data

Figure 6 shows the distribution of magnetic flux density along y-axis. The value is averaged in x-axis direction. In Fig. 6.(a), we can see that the magnetic flux density becomes asymmetrical distribution to the inclined defect. Furthermore, in Fig. 6.(b), we can observe the change deriving from the welded zone or HAZ.

Then, defect shape evaluation for the inclined defect was conducted by using magnetic dipole model and the inverse analysis based on the SVD technique. In this study, we assumed that the inclination angle of the defect is known in advance, because as for the defects like Type III around welded zone, they often generate along with the welded zone in many cases, and that inclined angle is

known in most cases. Therefore, the inverse analysis is conducted for the magnetic dipoles configured on the plane of inclination angle $\theta = 20^\circ$ ( $x - z'$ plane of Fig.2).

Figure 7 shows the magnitude of reconstructed magnetic dipoles on the $x - z'$ plane obtained by the inverse analysis. In this figure, black color corresponds to the high density area of magnetic dipoles, thus this means this area is defected. Similarly, white area corresponds to non-defected area. The boundary of the real defect is indicated as dotted lines (The depth is 2.5 mm as shown in Fig.2).

In Fig. 7(a), the magnitude in the area of $-0.5 \text{ mm} < z' < 0.0 \text{ mm}$ indicates almost zero, and this does not represent the characteristic of the surface defect. In our experience, this phenomenon often happens when the magnetic flux data for inverse analysis is obtained by experimental measurement, although this phenomenon does not happen when the magnetic flux data is obtained theoretically by numerical calculations as in equation (1)〜(3). However, this phenomenon happens only on the area of near $z' \approx 0$ mm. Thus, this does not have a bad influence on defect evaluation. On the contrary, in Fig. 7(b), the unsuitableness of the magnetic dipole magnitude abovementioned spreads far more widely. The reason is considered to be the influence of the welded zone. As a result, the black area crosses over the boundary of defect extensively. In contrast, the black area is above the boundary adequately in Fig.7(a). For these reasons, acceptable solution is obtained for case of applied magnetic field $4.88 \times 10^{-1}$T. Whereas, adequate result was not obtained in case of applied magnetic field $1.33 \times 10^{-1}$T.

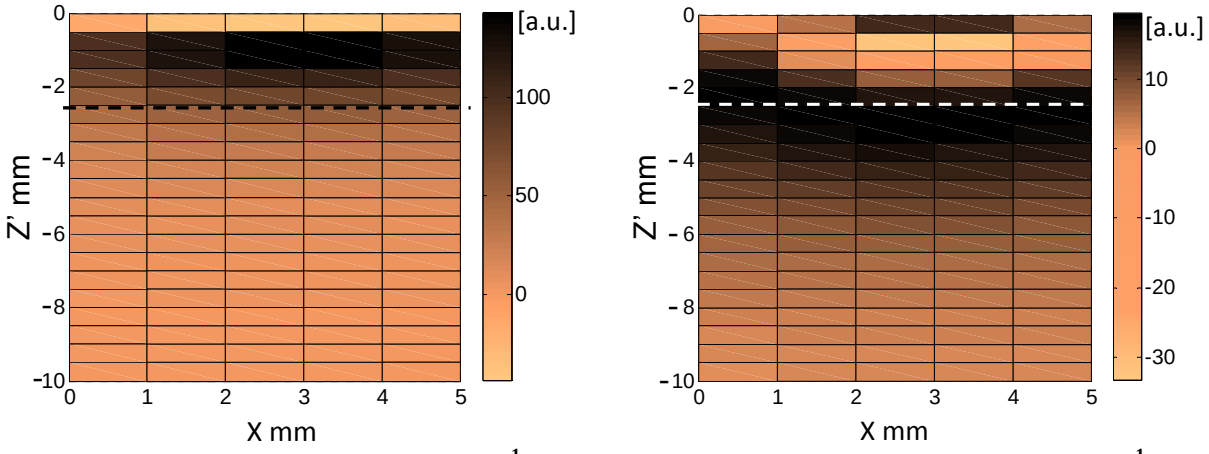


**(a) Applied magnetic field $4.88 \times 10^{-1}$T** **(b) Applied magnetic field $1.33 \times 10^{-1}$T**

**Fig. 7. Magnitude of reconstructed magnet dipoles of inverse analysis on the inclined plane (Dotted lines indicate the boundary of real defect)**

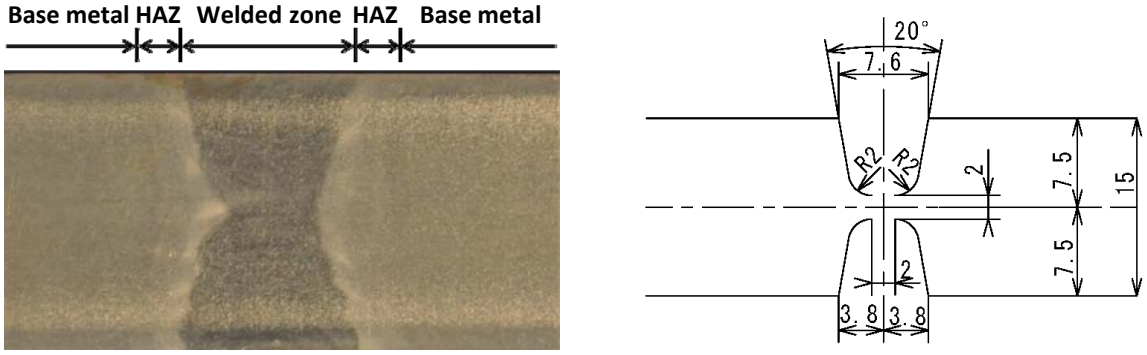


**Fig. 8. Welded zone of high chrome steel**

## 3.4. Result of inverse analysis using modified experimental data

In order to evaluate the influence of the welded zone on the magnetic flux distribution, the

magnetic property of that area was investigated. The magnetic property of the specimen which was cut out from the welded zone of the high chrome steel plate (shown in Fig. 8.) was measured by a Vibrating Sample Magnetometer (VSM), and the B-H curves for each material were obtained as shown in Fig.9. In the range of low magnetic field, permeability of the welded zone and HAZ were lower than that of base metal. Therefore, it seems that this discrepancy of permeability affected the distribution of magnetic flux density and this made the result of the inverse analysis unsuitable. On the other hand, in the range of saturated magnetization, there was almost no difference between both materials, and it seems that the inverse analysis was hardly affected.

Magnetic flux density distribution of the specimen in Fig. 8. was measured, and we subtracted this value from the distribution of Fig. 6.(b) as shown in Fig. 10. By this operation, we could remove the influence of welded zone, and we could obtain only the influence of the inclined defect.

Figure 11 shows the magnitude of reconstructed magnetic dipoles of the inverse analysis obtained from the magnetic flux distribution of Fig.10. In this case, adequate defect shape was obtained.

## 4. Conclusion

Magnetic flux density distribution of inclined defect around the welded zone of high chromium steel welded specimen was measured, and inverse analysis was conducted. Defect shape was obtained adequately from the magnetic flux density under the high magnetic field, without being subject to the influence of a welded zone. Under the low magnetic field, influence of welded zone became large relatively. However, by carrying out subtraction operation of the magnetic property, magnetic flux density distribution without influence of welded zone was extracted, and adequate defect shape was obtained by inverse analysis.

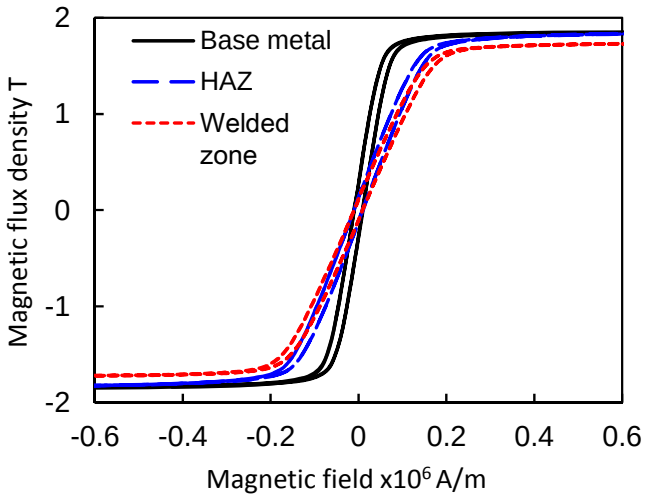


**Fig. 9. B-H Curve**

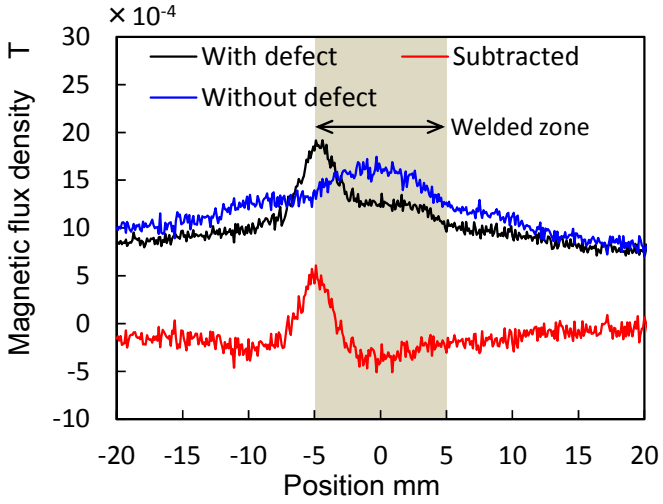


**Fig. 10. Magnetic flux leakage distribution**

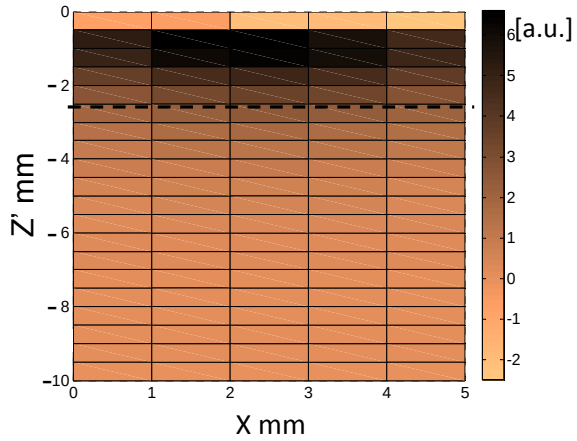


**Fig. 11. Result of inverse analysis using subtracted magnetic flux distribution**

## Acknowledgement

Present study includes the result of "Core R&D program for commercialization of the fast breeder reactor by utilizing Monju", entrusted to Universitiy of Fukui by the Ministry of Education, Culture, Sports, Science and Technology of Japan(MEXT), and reentrusted to National Institute of Advanced Industrial Science and Technology by University of Fukui at FY 2011.

## References

[1] T. Suzuki, A. Terasaki, A. Sasamoto, Y. Nishimura and T. Teramoto, Nondestructive evaluation of ferromagnetic structural materials using FG sensor, Electromagnetic Nondestructive Evaluation, (XII) (2009), 271-278.
[2] T. Suzuki, K. Hasumi, T. Kurota and T. Teramoto, Analysis and evaluation of cross-sectional shape for defect of SS400 using fluxgate sensor, Journal of JSAEM, 19 – 2 (2011), 342-347 (in Japanese).
[3] D. Minkov, J. Lee and T. Shoji, Study of crack inversions utilizing dipole model of a crack and hall element measurements, Journal of Magnetism and Magnetic Materials, 217 (2000), 207-215.
[4] D. Minkov and T. Shoji, Method for sizing of 3-D surface breaking flaws by leakage flux, NDT&E international, 31-5 (1998), 317-324.
[5] R. Baskaran and M. P. Janawadkar, Imaging defects with reduced space inversion of magnetic flux leakage fields, NDT&E international, 40 (2007), 451-454.
[6] R. Baskaran and M. P. Janawadkar, Defect localization by orthogonally projected multiple signal classification approach for magnetic flux leakage fields, NDT&E international, 41 (2008), 416-419.
[7] R. Baskaran and M. P. Janawadkar, Localization of defects in magnetic permeable bar by multiple signal

classification approach using rotating dipole model, NDT&E international, 42 (2009), 664-667.
[8] R. Baskaran and M. P. Janawadkar, Dipole identification and localization using pseudo-inverse techniques for magnetic flux leakage experiments, Electromagnetic Nondestructive Evaluation, (XV) (2012), 167-174.
[9] S. Nakasumi and T. Suzuki, Evaluation of defects based on inverse analysis considering the resolution of magnetic sensors, E-Journal of Advanced Maintenance, 3-1 (2011), 1-10.
[10] S. Nakasumi and T. Suzuki, Improvement of restoration accuracy of semi-elliptical surface crack considering the resolution of flux gate sensor, Electromagnetic Nondestructive Evaluation, (XV) (2012), 151-158.
[11] A. N. Tikhonov and V. Y. Arseine, Solutions of ill-posed problems, Halsted Press, 1977.
[12] C. Hansen, Analysis of discrete ill-posed problems by means of the L-Curve, Society for Industrial and Applied Mathematics, 34 - 4 (1992), 561-580.